Journal of Experimental Botany, Vol. 65, No. 13, pp. 3499–3511, 2014
doi:10.1093/jxb/eru169 Advance Access publication 8 May, 2014

Journal of Experimental Botany
www.jxb.oxfordjournals.org

RESEARCH PAPER

When do different C_4 leaf anatomies indicate independent C_4 origins? Parallel evolution of C_4 leaf types in Camphorosmeae (Chenopodiaceae)

Gudrun Kadereit[1,*], Maximilian Lauterbach[1], Michael D. Pirie[1,2], Rami Arafeh[3] and Helmut Freitag[4]

[1] Institut für Allgemeine und Spezielle Botanik und Botanischer Garten der Johannes Gutenberg-Universität Mainz, D-55099 Mainz, Germany
[2] Department of Biochemistry, University of Stellenbosch, Matieland 7600, South Africa
[3] Biotechnology Research Center, Palestine Polytechnic University, PO Box 198, Hebron, Palestine
[4] Institut für Biologie, Arbeitsgruppe Systematik und Morphologie der Pflanzen, Universität Kassel, D-34109 Kassel, Germany

* To whom correspondence should be addressed. E-mail: clausing@uni-mainz.de

Received 5 November 2013; Revised 11 March 2014; Accepted 21 March 2014

Abstract

Broad-scale phylogenetic studies give first insights in numbers, relationships, and ages of C_4 lineages. They are, however, generally limited to a model that treats the evolution of the complex C_4 syndrome in different lineages as a directly comparable process. Here, we use a resolved and well-sampled phylogenetic tree of Camphorosmeae, based on three chloroplast and one nuclear marker and on leaf anatomical traits to infer a more detailed picture of C_4 leaf-type evolution in this lineage. Our ancestral character state reconstructions allowed two scenarios: (i) *Sedobassia* is a derived C_3/C_4 intermediate, implying two independent gains of C_4 in *Bassia* and *Camphorosma*; or (ii) *Sedobassia* is a plesiomorphic C_3/C_4 intermediate, representing a syndrome ancestral to the *Bassia*/*Camphorosma*/*Sedobassia* lineage. In *Bassia*, a kochioid leaf type (*Bassia muricata* and/or *Bassia prostrata* type) is ancestral. At least three independent losses of water-storage tissue occurred, resulting in parallel shifts towards an atriplicoid leaf type. These changes in leaf anatomy are adaptations to different survival strategies in steppic or semi-desert habitats with seasonal rainfall. In contrast, *Camphorosma* shows a fixed C_4 anatomy differing from *Bassia* types in its continuous Kranz layer, which indeed points to an independent origin of the full C_4 syndrome in *Camphorosma*, either from an independent C_3 or from a common C_3/C_4 intermediate ancestor, perhaps similar to its C_3/C_4 intermediate sister genus *Sedobassia*. The enlarged bundle sheath cells of *Sedobassia* might represent an important early step in C_4 evolution in Camphorosmeae.

Key words: *Bassia*, bundle sheath, C_4 photosynthesis, *Camphorosma*, Kranz anatomy, *Sedobassia*, water-storage tissue.

Introduction

Phylogenetic inference methods present a powerful means of identifying putative shifts between C_3 and C_4 photosynthesis (Sage *et al.*, 2011, and references therein). If photosynthetic syndrome is treated as a single (functional) character with two states (either C_3 or C_4), it is straightforward to infer the number and timing of shifts between states in a given clade. On this basis, Christin *et al.* (2008) inferred numerous independent origins of C_4 and dated them to the Oligocene decline in atmospheric CO_2. However, the C_4 syndrome is both complex (comprising multiple individual adaptations) and diverse (the adaptations differ across clades), and may have originated in response to different selective pressures in

Abbreviations: cp, chloroplast; ITS, internal transcribed spacer; ML, maximum-likelihood; mya, million years ago.

different lineages (Osborne and Freckleton, 2009; Edwards and Smith, 2010; Kadereit *et al.*, 2012). It is therefore a considerable simplification to treat the highly complex C_4 syndrome as a single homologous character state (Christin *et al.*, 2010) and it may be misleading thereby to model the gain of that state as a single, directly equivalent process.

Treating C_3 versus C_4 pathways as a simple, discrete binary trait might lead to an overestimation of the number of C_4 origins if the evolutionary process involved intermediate, evolutionarily stable states (Sage *et al.*, 2012) or so-called precursors (Marazzi *et al.*, 2012). Such a C_3/C_4 intermediate common ancestor, or simply an ancestor with a certain feature that facilitated the evolution of the C_4 pathway, might have given rise to several, not strictly independent C_4 lineages (Christin *et al.*, 2010; Christin and Osborne, 2013). Hence, in assessing the homology of C_4 across lineages we need to consider the genetic and phenotypic basis of the different individual traits involved. Bundle-sheath anatomy, interveinal distance, and organelle composition of bundle-sheath cells of C_3 relatives have been proposed as key traits for understanding C_4 evolution (Sage, 2001; McKown and Dengler, 2007). Griffiths *et al.* (2013) put forward the idea that functions of the bundle sheath, in particular the maintenance of leaf hydraulic continuity, were under selective pressure in more seasonal climates and that an increase in bundle sheath/mesophyll ratio subsequently also proved advantageous for C_4 evolution. This is supported by a study of multiple leaf anatomical traits in grasses by Christin *et al.* (2013) who showed that C_4 evolvability significantly increased in lineages with a bundle-sheath proportion of >15% resulting from a combination of shorter interveinal distances and larger bundle-sheath cells.

It is conceivable that a proportion of the numerous non-grass C_4 lineages also stem from ancestors with common traits that in 'evolutionary retrospect' appear as pre-adaptations to C_4 evolution. However, traits that increase C_4 evolvability in grasses do not necessarily apply universally across different lineages. Succulent C_4 groups characterized by water-storage tissues in leaves or stems exhibit very different leaf anatomies to those of C_4 grasses. In Chenopodiaceae, there is strong evidence that, in succulent C_4 lineages, succulence evolved before C_4 photosynthesis (Schütze *et al.*, 2003; Kadereit *et al.*, 2012). Preliminary data from other succulent C_4 lineages such as Sesuvioideae (Aizoaceae) and *Zygophyllum* (Zygophyllaceae) also indicate that C_3 ancestors of C_4 lineages showed water-storage tissue (G. Kadereit, unpublished results). Kadereit *et al.* (2012) concluded that drought tolerance achieved by water storage is an important adaptation that enhanced the evolution of C_4 photosynthesis in these chenopod lineages.

However, forms of water storage and leaf anatomy in general differ dramatically across different succulent C_4 groups. Of the 14 general types of C_4 leaves described for eudicots (summarized by Edwards and Voznesenskaya, 2011), three (atriplicoid, simplicifolioid, and isostigmoid) do not show significant water-storage tissue, while the remaining 10 types (kochioid, salsoloid, salsinoid, schoberioid, Kranztecticornioid, pilosoid, portulacelloid, glossocardioid, and the two single-cell C_4 leaf types of *Bienertia* and *Suaeda aralocaspica*) are characterized by a variety of distinct patterns of tissues dedicated to water storage (see Figs 3 and 4 in Edwards and Voznesenskaya, 2011). The types differ mainly in the position and amount of water-storage tissue, the position and orientation of vascular bundles, the presence or absence of a hypodermis, and the position of the photosynthetic carbon reductive (PCR) tissue in relation to the vascular tissue (Edwards and Voznesenskaya, 2011, and references therein).

The diversity of C_4 syndromes in succulent lineages could thus be interpreted in a number of different ways. A pre-adaptation (evolutionary precursor) scenario might invoke diversifications within C_4 lineages resulting in distinctly differentiated leaf types that nevertheless stem from a common C_4 or C_3/C_4 intermediate ancestor. By contrast, the diversity of C_4 anatomy has been interpreted as evidence for multiple independent origins from different (extinct) C_3 ancestors. For example, Schütze *et al.* (2003) argued that the *Schoberia* and *Salsina* leaf types of *Suaeda* (Chenopodiaceae), although sister groups, represent independent C_4 origins due to their fundamentally different C_4 anatomies. This conclusion was later supported by developmental and biochemical (Koteyeva *et al.*, 2011) as well as phylogenetic (Kapralov *et al.*, 2006) studies. It is even conceivable that selective pressure, for example for drought resistance, might lead to convergence of similar leaf types (and perhaps also C_4) in independent lineages. Hence, to accurately assess the numbers of independent gains of C_4 photosynthesis in groups such as Chenopodiaceae it is important to dissect C_4 anatomy into its constituent traits and infer the sequence of acquisition of these traits using phylogenies with exhaustive representation of both C_4 and closely related C_3 lineages.

The study group investigated here, the Camphorosmeae (Chenopodiaceae), occurs in steppes, semi-deserts, salt marshes, and disturbed places of Eurasia, South Africa, North America, and Australia. Camphorosmeae consist of subshrubs and annuals, mostly with moderately to strongly succulent leaves with a central aqueous tissue. Only a few species show flat leaves and lack a water-storage tissue (Freitag and Kadereit, 2014). The tribe consists of three major lineages, two of them performing C_3 photosynthesis and one C_4 lineage (Kadereit and Freitag, 2011).

One C_3 lineage (*Sclerolaena* clade) comprises the species-rich monophyletic clade of Australian Camphorosmeae, which contains the large genera *Sclerolaena* and *Maireana* and which is sister to the small Central Asian genus *Grubovia* (Cabrera *et al.*, 2011). The *Sclerolaena* clade rather consistently shows the *Neokochia* leaf type with a central water-storage tissue, one large central vascular bundle, and many small peripheral vascular bundles at the border to a multilayered chlorenchyma (Freitag and Kadereit, 2014). The other C_3 lineage (*Chenolea* clade) consists of five disjunctly distributed relict species, the North American genus *Neokochia* (two species), the South African *Chenolea* (two species), the Mediterranean narrow endemic *Eokochia* (one species), and the Eurasian widespread *Spirobassia* (one species; Kadereit and Freitag, 2011). Among these, two new C_3 leaf types were found, the *Eokochia* type with complex lateral vascular bundles and the *Chenolea* type with all bundles in one plane, embedded in massive aqueous tissue, and a peripheral

fenestrate chlorenchyma. *Neokochia* and *Spirobassia* show the *Neokochia* type. Symplesiomorphies of the C_3 leaf types are isobilateral organization, multilayered chlorenchyma, central water-storage tissue, and absence of a hypodermis (Freitag and Kadereit, 2014).

The C_4 lineage (*Bassia* clade) comprises 25 species in three genera, *Bassia* (20 species), *Camphorosma* (four species), and *Sedobassia* (one species), and is mainly distributed in Eurasia, with just two species of *Bassia* occurring in South Africa (Kadereit and Freitag, 2011; Akhani and Khoshravesh, 2013; Freitag and Kadereit, 2014). *Bassia* and *Camphorosma* include only C_4 species, while *Sedobassia* represents a C_3/C_4 intermediate recently identified on the basis of leaf anatomy (Kadereit and Freitag, 2011; Freitag and Kadereit, 2014), gas exchange analysis, and immunolocalization of glycine decarboxylase (Voznesenskaya *et al.*, 2013; Sage *et al.*, 2014, this issue). If C_4 is treated as a simple binary character, and *Sedobassia* as C_3 rather than C_4, then the tree topology might suggest two potential scenarios for C_4 evolution in Camphorosmeae: a single gain of C_4 in the common ancestor of the *Bassia*/*Camphorosma*/*Sedobassia* lineage with (partial) loss in the C_3/C_4 intermediate *Sedobassia*, or two independent gains in *Bassia* and *Camphorosma*, plus one—only partially accomplished—in *Sedobassia*. A parsimonious interpretation would favour the former scenario, while the latter would be favoured if losses of C_4 are assumed to be less likely than independent gains, as argued by Christin and Osborne (2013, and references therein). Freitag and Kadereit (2014) indeed argued in favour of three independent origins but based on leaf anatomical characters rather than the probability of C_4–C_3 reversals per se.

Species of the *Bassia* clade can be assigned to five different C_4 leaf types, not counting the *Sedobassia* C_3/C_4 intermediate leaf type, which differs from all others in having an undifferentiated multilayered chlorenchyma (as do the C_3 species) but shows enlarged bundle sheath cells (Fig. 1A). All species of *Camphorosma* are consistent in showing only one C_4 leaf type (*Camphorosma* type) with one continuous layer of palisade cells [photosynthetic carbon assimilative (PCA) tissue] in close contact with one continuous layer of Kranz cells (photosynthetic carbon reductive tissue) beneath a hypodermis (Fig. 1B). In contrast, *Bassia* includes four different C_4 leaf types. The *Bassia prostrata* type and *Bassia muricata* type show a mostly continuous layer of photosynthetic carbon assimilative tissue and Kranz cells in arch- or fan-shaped groups, all in direct contact with the vascular bundles. They differ in the presence/absence of a hypodermis (Fig. 1C–J). The *Bassia lasiantha* type and *Bassia eriantha* type both show an atriplicoid arrangement of the photosynthetic carbon assimilative and reductive tissues but also differ in the presence/absence of a hypodermis (Fig. 1K; see also Fig. 3B in Akhani and Khoshravesh, 2013).

Tracing the evolution of C_4 leaf anatomy in the *Bassia* clade was hampered in previous studies (Kadereit and Freitag, 2011; Freitag and Kadereit, 2014) by a partly unresolved phylogenetic tree and the lack of a few important species. Here, we present a fully resolved and nearly complete molecular phylogeny of the *Bassia* clade based on three chloroplast (cp) markers (the *atpB-rbcL* spacer, *rpl*16 intron, and *ndhF-rpl*32 spacer) and the nuclear ribosomal internal transcribed spacers (ITS), and the results of leaf anatomical sectioning for all terminals in the tree. We inferred and tested models describing the sequence and number of acquisitions of C_4 using ancestral state reconstruction approaches that treated the different individual leaf anatomical characteristics as individually independent or linked elements of a complex C_4 syndrome. We tested the hypotheses of three independent C_4 origins and multiple (potentially associated) losses of water-storage tissue and hypodermis in the *Bassia* clade raised in Freitag and Kadereit (2014) and critically assessed the assumption that different C_4 leaf types are necessarily indicative of independent C_4 origins.

Materials and methods

Plant material and sampling

We mainly used herbarium material for the molecular and anatomical studies. In a few cases, we used plants raised in the greenhouse from seeds collected in the wild. Voucher information for all accessions is given in Supplementary Table S1 (available at *JXB* online). Sampling of the *Bassia* clade (including *Bassia*, *Camphorosma*, and *Sedobassia*) was complete except for one dubious species, *Bassia aegyptiaca* (see Kadereit and Freitag, 2011). We included multiple accessions for most species to ensure species monophyly and to improve upon our previous assessment of intraspecific variation of anatomical characters. *Chenolea convallis* (Snijman and Manning, 2013), *Bassia littorea* (Kadereit and Freitag, 2011) and *B. eriantha* (Akhani and Khoshravesh, 2013) have not been included in our previous molecular data sets.

Sequencing and phylogenetic inference

In total, 79 accessions were included in the phylogenetic analyses representing the three genera of the *Bassia* clade (*Bassia*, *Camphorosma*, and *Sedobassia*) with 25 species and seven species of the remaining Camphorosmeae. Supplementary Table S1 (available at *JXB* online) gives an overview of the samples included, sequences newly generated for this study, sequences included from previous studies, and missing data. *Salsola genistoides* was selected as outgroup representing a basal representative of Salsoloideae (Kadereit and Freitag, 2011). Total DNA was extracted from 20 mg of dried leaf material using a DNeasy Plant Mini kit (Qiagen) following the manufacturer's specifications. PCR was carried out in T-Professional or T-Gradient Thermocycler (Biometra). The ITS region was amplified with an Applied Biosystems Thermal Cycler model 2720. Supplementary Table S2 (available at *JXB* online) gives the details of primer sequences, PCR components, and cycler programme for each marker. PCR products were checked on 1% agarose gels and subsequently purified using a NucleoSpin® Gel and PCR Clean-up kit (Macherey-Nagel) following the manufacturer's instructions. The ITS amplicons were purified with an AccuPrep® PCR Purification kit (Bioneer). DNA sequences were obtained using a Big Dye® Terminator v3.1 Cycle Sequencing kit (Applied Biosystems) in combination with the primers mentioned above following a purification step using IllustraTM SephadexTM G-50 Fine DNA Grade (GE Healthcare). DNA fragments were sequenced using an automatic capillary sequencer GA3130XL (Applied Biosystems) following the Sanger method. Forward and reverse sequences were edited and merged to consensus sequences, which then were aligned using Sequencher 4.1.4 (Gene Codes Corp.) and MEGA5 (Tamura *et al.*, 2011). All alignments were checked and corrected manually.

For the ITS data set, for the combined three cp markers and for the combined ITS+cp data, maximum-likelihood (ML) phylogenetic

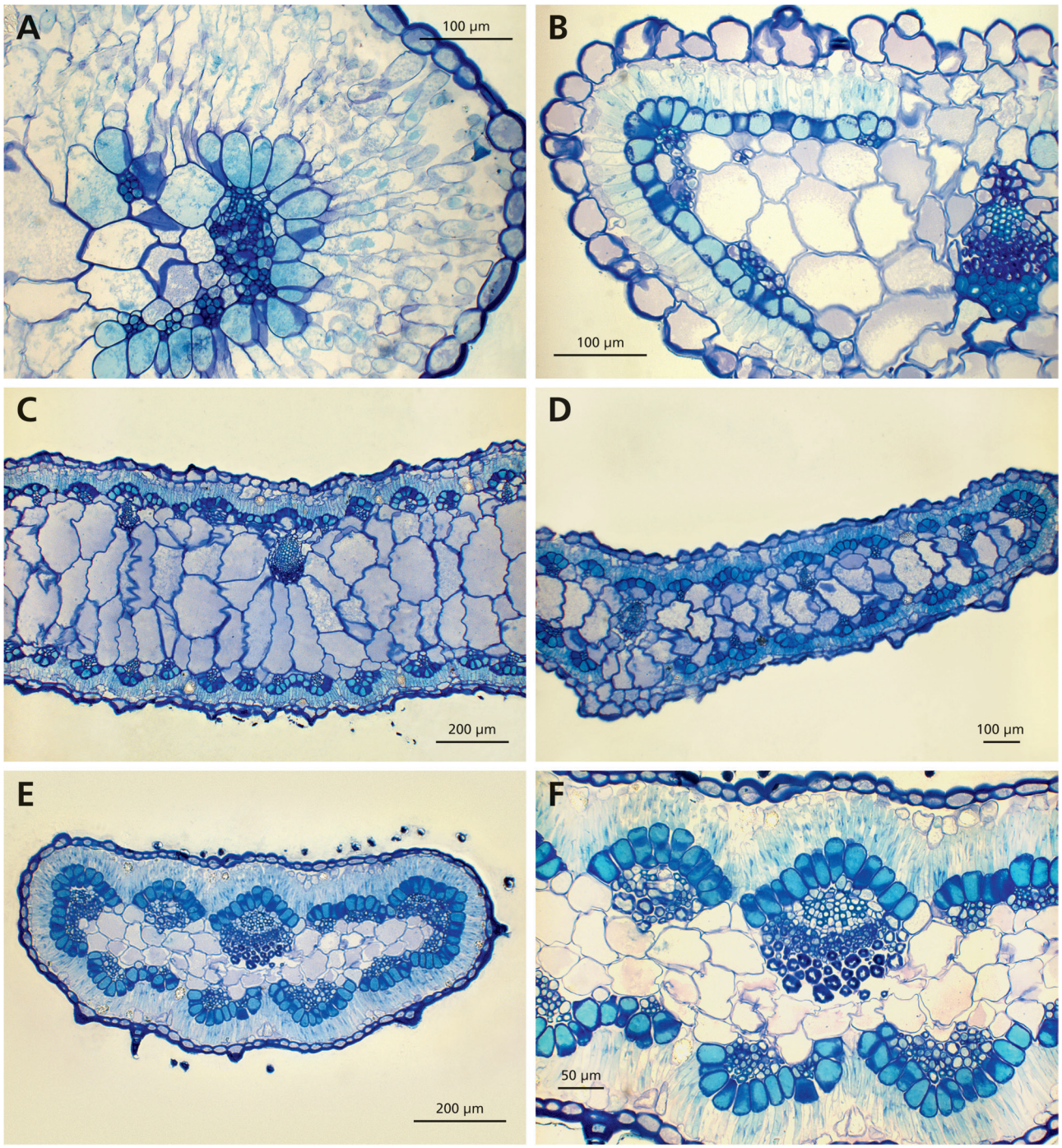

Fig. 1. Leaf cross-sections of *Sedobassia*, *Camphorosma*, and *Bassia* (sample numbers refer to voucher information given in Supplementary Tables S1 and S3 available at *JXB* online). (A) *Sedobassia sedoides* (chen 2462), *Sedobassia* type. (B) *Camphorosma annua* (chen 358), *Camphorosma* type. (C) *Bassia hyssopifolia* (chen 150), *Bassia prostrata* type. (D) *Bassia littorea* (chen 1879), *B. prostrata* type. (E, F) *B. prostrata* (chen 2719), *B. prostrata* type. (G–H) *Bassia stellaris* (chen 135), *Bassia muricata* type. (I) *B. muricata* (chen 2447), *B. muricata* type. (J) *Bassia scoparia* (chen 2722), *B. muricata* type. (K) *B. scoparia* (chen 2449), *Bassia lasiantha* type. (L) *Bassia salsoloides* (chen 2464), *B. prostrata* type.

analyses were performed using RaxML on Cipres (Stamatakis, 2006; Stamatakis *et al.*, 2008; Supplementary Figs S1–S3 available at *JXB* online), including bootstrapping that was halted automatically following the majority-rule 'autoMRE' criterion. Parsimony bootstrapping was performed using PAUP* (Swofford, 2003) with 10 000 replicates of a single random-addition sequence and tree bisection and reconnection, saving a single tree each replicate (following Müller, 2005).

A chronogram was generated using BEAST v.1.5.4 (Bayesian Evolutionary Analysis by Sampling Trees; Drummond and Rambaut, 2007, Rambaut and Drummond, 2003). The BEAST xml input files (available from the corresponding author upon request) were created with BEAUti v.1.5.4 (Drummond and Rambaut, 2007). Monophyly of the ingroup (all accessions except *Salsola genistoides*) was constrained in order to root the tree and put an age constraint on the ingroup node. The substitution model parameters were set to GTR+G with four categories for G. A relaxed-clock model was implemented in which rates for each branch were drawn independently from a log-normal distribution and a birth and death

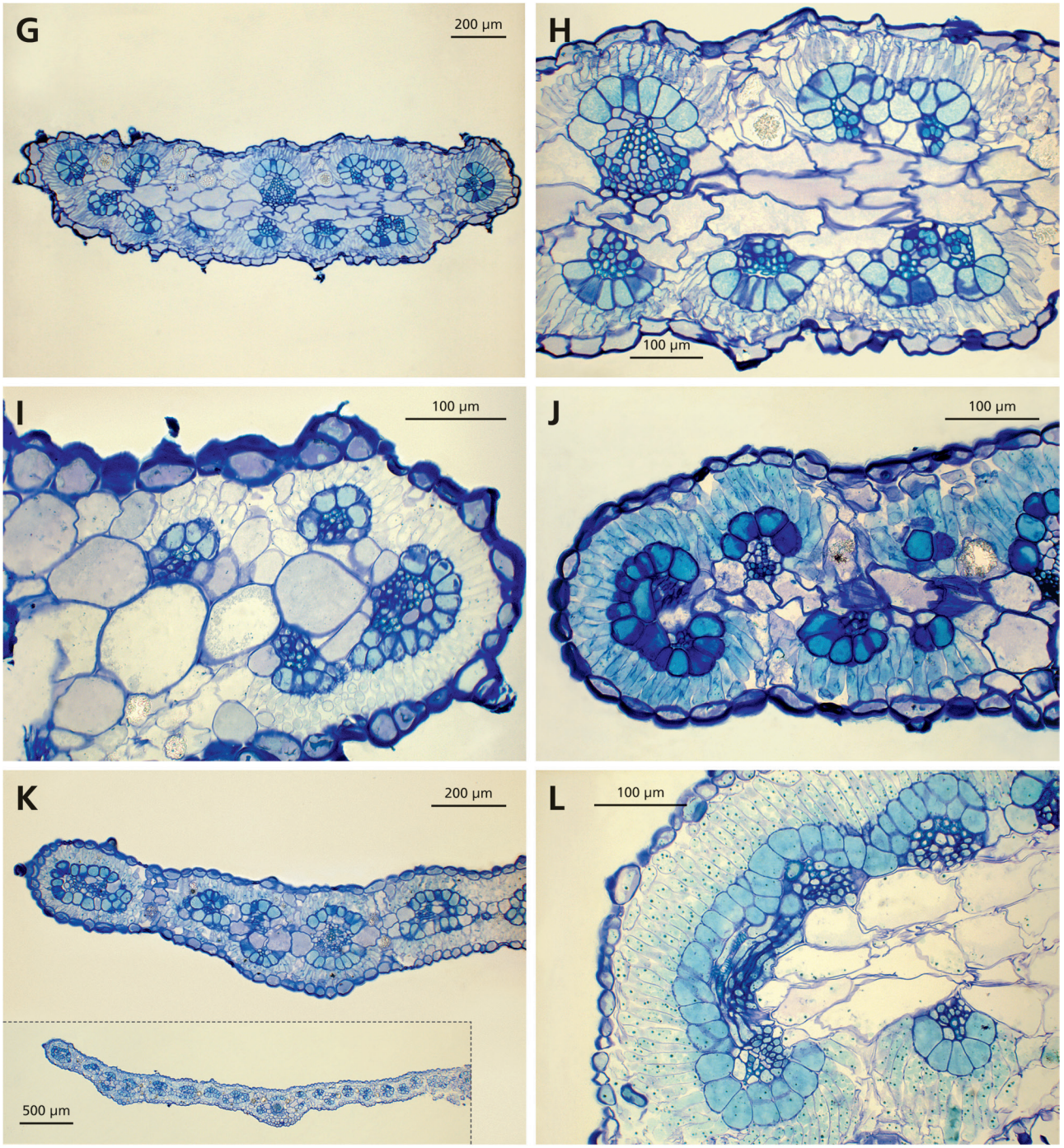

Fig. 1. Continued

demographic model was assumed. We used results from a previous family-wide dating (Kadereit *et al.*, 2012) to constrain the age of the crown node of Camphorosmeae with the 95% confidence interval of 29–15 million years ago (mya) assuming a uniform distribution. The Markov chain Monte Carlo method was initiated on a random starting tree. Two independent runs of 20 000 000 iterations were performed with a sampling frequency of 1000. Topological convergence was confirmed using AWTY (Wilgenbusch *et al.*, 2004) and convergence of model parameters was confirmed using TRACER (Rambaut and Drummond, 2003). The first 1000 trees were discarded. Posterior probability clade support was calculated together with the medians and 95% confidence limits for ages of the nodes from the remaining 19 000 trees. A subset of 1901 trees and the resulting maximum clade credibility chronogram was used in the character optimizations (see below).

Anatomical studies, character coding, and ancestral character state reconstruction

The leaf anatomy of 20 accessions included here was studied in Freitag and Kadereit (2014) and four in Akhani and Khoshravesh (2013; compare Supplementary Table S1 available at *JXB* online). Leaves of the remaining 57 accessions were sectioned after embedding in Technovit 7100 (Heraeus-Kulzer) using the following method: herbarium material was soaked for 7–10 d in 10% ammonia

solution, and fresh material (a few accessions only) was hardened in formaldehyde/acetic acid/ethanol at least overnight. Dehydration followed using an ascending ethanol series [15 (optional), 30, 50, 60, 70, 80, 90, and 96%], each step lasting at least 1 h. Fresh material started at 70% ethanol and soaked material at 15/30% ethanol. All embedding steps followed the manufacturer's protocol for Technovit 7100. Samples were incubated for 1–2 h or longer in pre-infiltration (Technovit 7100 liquid: absolute/96% ethanol, 1:1) and underwent 12 h or more of infiltration (liquid+hardener I). Only after complete polymerization (infiltration+hardener II) was sectioning started with a rotary microtome at 5–10 µm.

For staining, the following components were prepared separately: 0.004 g of Azur II (Sigma-Aldrich) was dissolved in 11 ml of distilled water; 0.008 g of eosin Y (Sigma-Aldrich) was dissolved in 11 ml distilled water, and 6 g of methylene blue was dissolved in 400 ml 96% ethanol and made up to 2000 ml with distilled water. The solutions of Azur II, eosin Y, and methylene blue were mixed with distilled water at a ratio of 26:26:22:26 of the desired volume of dye. The dye was applied to the slides for 6–8 min. They were then washed with distilled water and briefly rinsed with 96% ethanol and again with distilled water. If the staining was not convincing after the first attempt, it was possible to stain the slides again.

The following traits were coded in a matrix of discrete character states:

1. Photosynthetic type was coded according to carbon isotope measurements given in Freitag and Kadereit (2014, and references therein): C_3=0, C_4=1.
2. Water-storage tissue was coded as present when at least one full layer of water-storing cells was present in the centre of the leaf. An interrupted layer or only a few large cells was therefore coded as absent (compare Fig. 1K): present=0, absent=1.
3. A hypodermis was only coded as present when a layer of hypodermis cells completely surrounding the leaf was present (compare Fig. 1B, C). It was coded as absent when entirely so, or when only a few hypodermal cells were present (compare Fig. 1H, J): absent=0, present=1. The C_3 species (including *Sedobassia*), which all lack a hypodermis, were coded either as hypodermis absent (=0; coding A) or, in separate analyses, as hypodermis present (=1; coding B) in order to test the result given the hypothesis that the hypodermis of the C_4 species is homologous to the outer chlorenchyma layer of the C_3 species.
4. The position of chlorenchyma layers in relation to the vascular bundles was coded as follows: chlorenchyma not orientated towards the vascular bundle but in continuous layers=0, chlorenchyma (at least the inner layer) orientated towards the vascular bundle (Kranz-like or semi-Kranz-like)=1. For illustration of this character, see Fig. 1B (continuous Kranz layer) and Fig. 1E, F (interrupted Kranz layer).

Ancestral state reconstruction

In order to infer ancestral states for each of the characters independently, individual optimizations were performed on the binary characters under parsimony and ML in Mesquite over 1000 post-burnin trees from the BEAST analysis summarized on the maximum clade credibility tree. Under ML, the fit of single versus two-rate models given the maximum clade credibility tree was tested using a likelihood ratio test comparing to χ^2 distribution with 1 degree of freedom.

In order to simultaneously infer the sequence of evolution of combinations of character states, multistate character optimization was performed using (i) the observed, and (ii) all possible (ancestral) combinations of states as the multiple states of single characters. Parsimony optimizations were performed in Mesquite, applying step matrices to represent the number of character state changes implied by shifts between each pair of states (including those not observed in extant taxa; Supplementary Fig. S4 available at *JXB* online). For (ii), two combinations of characters were used: all four binary characters, yielding 16 possible combinations of states ('syndromes'; of which seven or nine, depending on the interpretation of the hypodermis character, are observed in extant taxa), and three, excluding the hypodermis character, yielding eight possible combinations (of which five are observed in extant taxa). The former was performed with both possible coding strategies for the hypodermis character. With this large number of character states combined with a relatively small number of state shifts, analysing this model under likelihood was deemed impractical and unnecessary.

Results

Phylogenetic inference

The combined data matrix included 3646 aligned positions (ITS region: 666 bp, *atpB-rbcL* spacer: 739 bp; *rpl*16 intron: 868 bp; *ndhF-rpl*32 spacer: 1373 bp). The data set contained a total of 1125 variable positions (ITS: 280; *atpB-rbcL* spacer: 152; *rpl*16 intron: 205; *ndhF-rpl*32 spacer: 488). The individual ML analyses of the ITS data set and the cp marker data set showed no conflicts in topology for nodes subject to bootstrap support ≥75% (Supplementary Figs S1 and S2 available at *JXB* online). The addition of the ITS data set to the cp data set resulted in improved bootstrap support values in most cases and no decrease in support >10%. The resulting combined tree was well resolved, especially with regard to deeper nodes (Supplementary Figs S2 and S3 available at *JXB* online). The results of the BEAST analysis are shown in Fig. 2.

Anatomical studies

Anatomical leaf types as defined in Freitag and Kadereit (2014) and summarized in the introduction were found to be consistent for most species (Figs 1 and 2, and Supplementary Table S3 available at *JXB* online). *Bassia indica*, *Bassia pilosa*, and *Bassia scoparia* showed variable leaf types with two different anatomical types occurring in each of these species (Supplementary Table S3 available at *JXB* online). Intermediate phenotypes were observed only in *B. prostrata*/*B. muricata* types (Fig. 1H, J) and *B. muricata*/*B. lasiantha* types (Fig. 1K), as reported previously by Freitag and Kadereit (2014).

Ancestral character state reconstruction

Individual parsimony optimizations of the four binary traits showed a small number of shifts in C_3/C_4 and Kranz-like arrangement of chlorenchyma layers in relation to the vascular bundles (both one to two gains and zero to one losses) and water-storage tissue (three losses) but a larger number of shifts between the presence and absence of a hypodermis (one to nine gains and zero to six losses). Under ML, the data for C_3/C_4, hypodermis absent/present (coding A) and bundle-sheath position best fitted a single rate model, while those for water-storage tissue and hypodermis (coding B) best fitted two-rate models (P<0.001 and P<0.005, respectively).

Optimizations of binary characters individually indicated that the *Bassia* clade was ancestrally succulent (parsimony 100% of reconstructions; ML: 77%, 23% equivocal) but equivocal for C_3/C_4 (parsimony: 100%; ML: 98%) and position

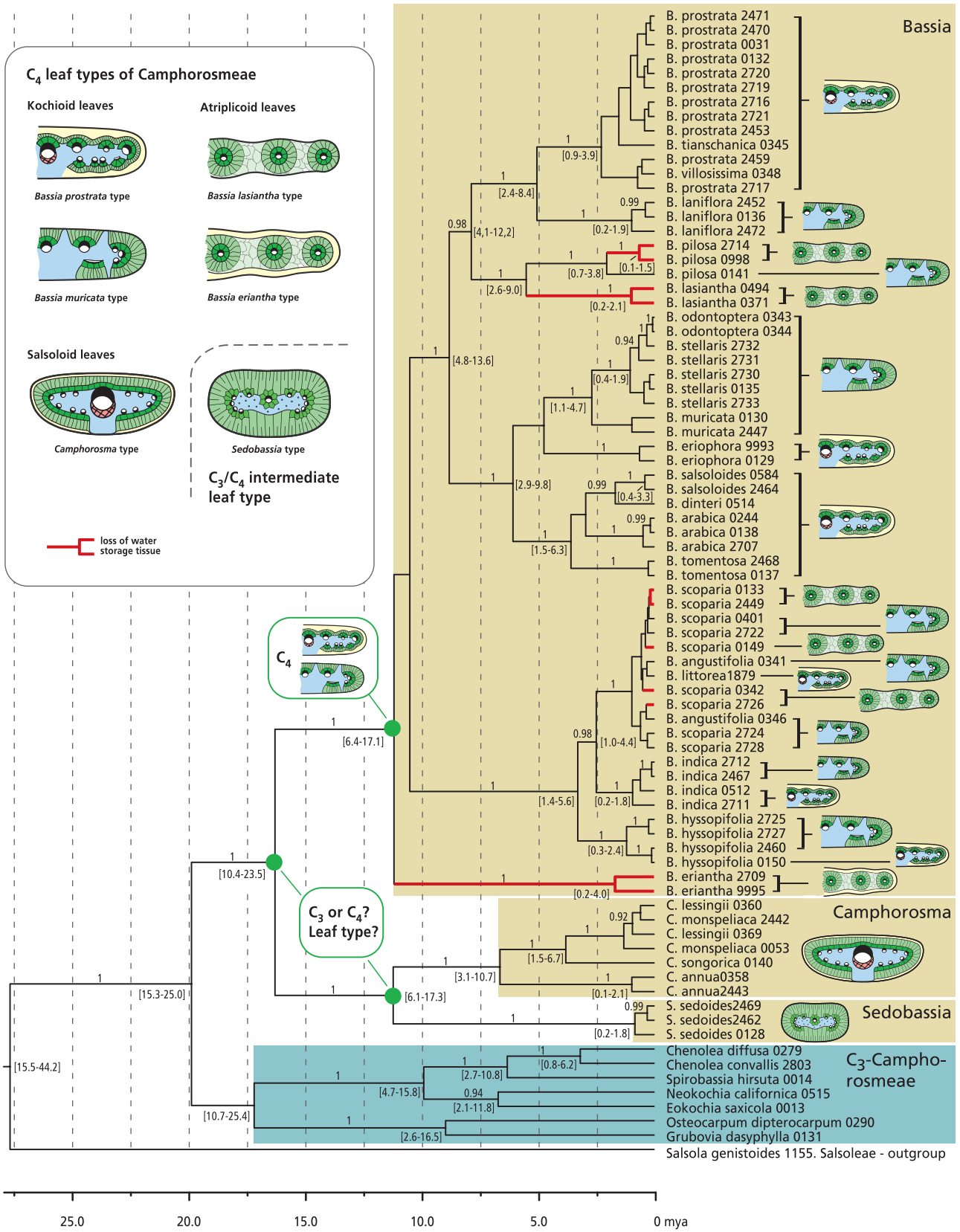

Fig. 2. Chronogram of Camphorosmeae (Chenopodiaceae) generated using BEAST v.1.5.4 based on three cp markers (*atpB-rbcL* spacer, *rpl*16 intron, and *ndhF-rpl*32 spacer) and the nuclear ribosomal ITS and 79 accessions of Camphorosmeae representing 32 species. The tree was rooted with *Salsola genistoides* (Salsoleae s.s.). Numbers above branches represent posterior probabilities and numbers in square brackets indicate 95% confidence intervals of the respective node ages.

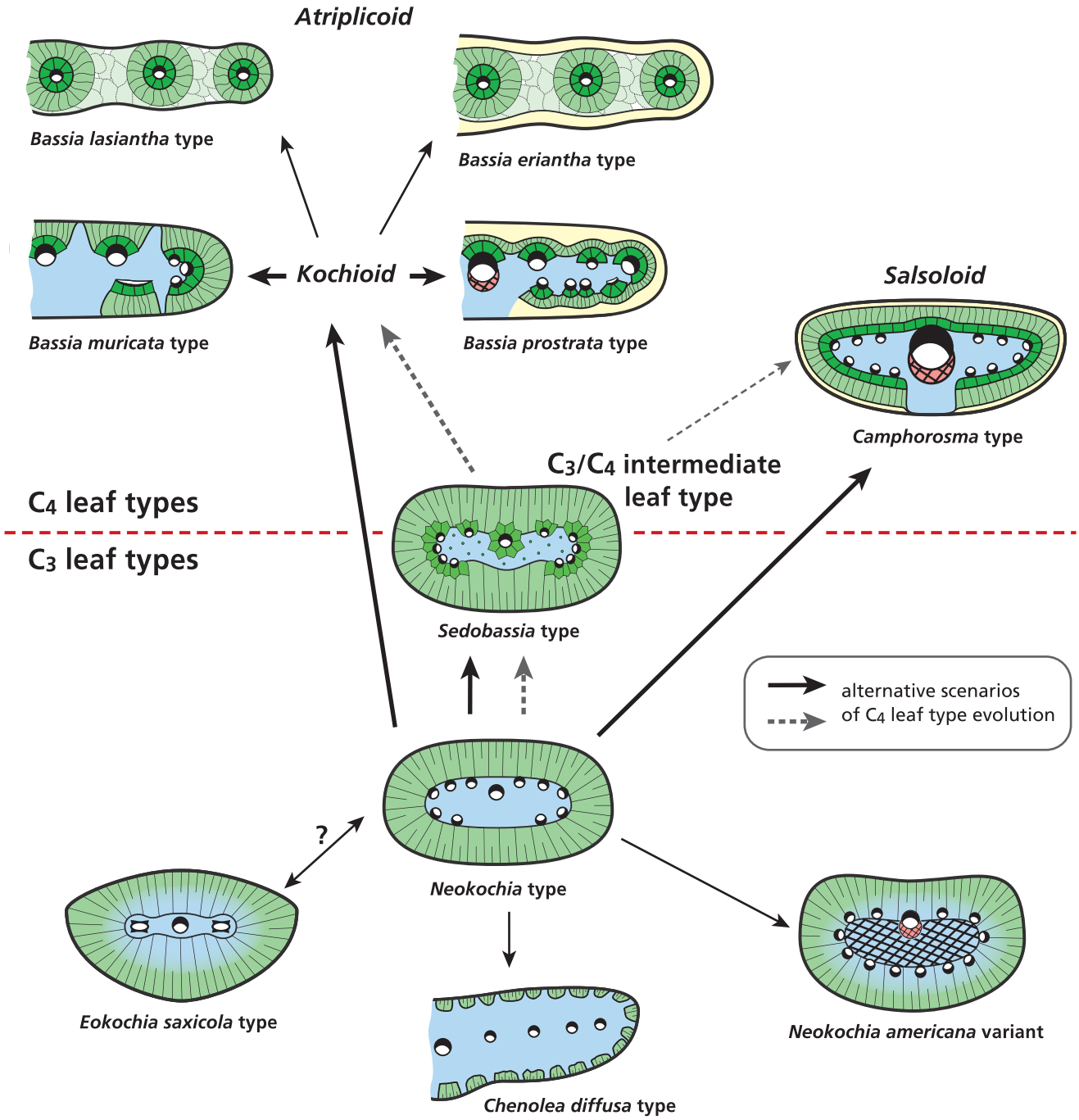

Fig. 3. Revised model of leaf type evolution in Camphorosmeae.

of Kranz cells (parsimony: 100%; ML: 95%). The inferred states for the presence/absence of a hypodermis in the most recent common ancestor of *Bassia* and that of *Sedobassia* and *Camphorosma* depended on the coding of outgroups and *Sedobasssia* under parsimony (present when the hypodermis is assumed to be homologous with the outer of multiple layers of chlorenchyma; absent when not), but were ambiguous under ML. Under both methods, ancestral states for this character were generally uncertain within the *Bassia* clade. The ancestral state reconstructions are summarized in Fig. 2.

Parsimony optimizations of multistate characters employing step matrices yielded results consistent with those of the binary characters individually. Although all combinations of ancestral states could in principle have been inferred, the parsimonious solutions for ancestral nodes included only those observed in extant taxa. The ancestral states of the *Bassia* clade and of *Sedobassia* and *Camphorosma* remained ambiguous, and hence on this basis neither the scenario of multiple gains of C_4 nor that involving both gain and loss can be rejected. However, when the eight-state coding was applied (excluding the hypodermis character), ancestral states within *Bassia* were largely unambiguously inferred as *B. muricata*/*B. prostrata* type (i.e. C_4, succulent, and with Kranz-like anatomy),

from which *B. lasiantha*/*B. eriantha* non-succulent types originated on at least three occasions.

Discussion

New insights into the phylogeny and taxonomy of Camphorosmeae

The molecular phylogeny presented here was based on the nuclear marker ITS and three cp markers and delivered improved resolution of the *Bassia* clade compared with our previous analysis (Kadereit and Freitag, 2011), which was based on ITS data only. The inclusion of multiple accessions for each species supports the monophyly of many species and supports our previous taxonomic judgements (Fig. 2). Nevertheless, a reassessment of species delimitation is still warranted within clades containing critical taxa such as the *B. scoparia* complex (including *B. littorea*, sequenced here for the first time, and *Bassia angustifolia*), the *B. prostrata* complex (including *Bassia tianschanica* and *B. villosissima*), the *stellaris stellaris* complex (including *Bassia odontoptera*), the *B. pilosa* complex (including *B. lasiantha*; compare Supplementary Fig. S3 available at *JXB* online), and the *Camphorosma monspeliaca* complex (including *Camphorosma lessingii*). Concerning *B. indica*, the absence of a hypodermis in the two samples from northern Africa and Jordan suggests that it may be appropriate to recognize two otherwise cryptic taxa within this species.

Our results support those of Akhani and Khoshravesh (2013) that *B. eriantha* is not closely related to *Bassia eriophora* with which it is easily confused (Kadereit and Freitag, 2011). *B. eriantha* is weakly supported as a sister group to the remaining species of the genus, within which *B. eriophora* is nested (see Supplementary Figs S1–S3 available at *JXB* online). The results also indicate the sister-group relationship of the recently described narrow endemic *Chenolea convallis* from southern Africa with the only other species of the genus, *Chenolea diffusa*. This is despite their marked differences in habit (truly subshrubby versus perennial herbaceous in *Chenolea diffusa*) and leaf anatomy (neokochioid versus *Chenolea type* in *Chenolea diffusa*). The unique characters of *Chenolea diffusa*, including its most peculiar leaf anatomy, are best interpreted as autapomorphies.

The centre of *Bassia* clade diversity is in West Asia and, given the phylogeny, it seems likely that all three genera (*Bassia*, *Sedobassia*, and *Camphorosma*) originated in that region. While the origin of *Bassia* dates back to the Early to Middle Miocene (23.5–10.4 mya), *Sedobassia* and *Camphorosma* separated during the Middle to Late Miocene (17.3–6.1 mya). The two South African species of *Bassia* (*Bassia salsoloides* and *Bassia dinteri*) form a monophyletic group and are most closely related to *Bassia arabica* and *Bassia tomentosa* (Fig. 2). These three lineages separated during the Pliocene (confidence interval 6.3–1.5 mya). *Bassia tomentosa* and *B. arabica* are prostrate subshrubs with a dense indumentum of appressed silky hairs, distributed in semi-desert communities along the northern margin of the Saharo-Sindian floristic region (Kadereit and Freitag, 2011). The two South African species are morphologically and ecologically distinct. *Bassia salsoloides* can be found along temporarily dry rivers of the Nama-Karoo, while *B. dinteri* is a rare plant in the fog desert of the Namib. These four species represent another example of Saharo-Sindian/South African disjunct distributions of arid-adapted clades (Verdcourt, 1969; Jürgens, 1997; Bellstedt *et al.*, 2012).

Most species of the above-mentioned species complexes of the *Bassia* clade (including *Bassia*, *Camphorosma*, and *Sedobassia*) originated during the Late Miocene to Pliocene (10–2 mya) with *Sedobassia sedoides* and *B. eriantha* being the only two exceptions. The stem lineages of these two species date back to the Middle to Late Miocene (17–6 mya; Fig. 2). This indicates that diversification within *Bassia* and *Camphorosma* coincides with the expansion of C_4 grasslands and steppes during the Late Miocene (Osborne and Beerling, 2006). The acquired C_4 pathway in *Bassia* and *Camphorosma* may have acted as a selective advantage under increasingly dry conditions and facilitated diversification in the expanding dry habitats (Kadereit *et al.*, 2012).

Origins of C_4 photosynthesis in Camphorosmeae

Our analysis showed that neither of the two possible scenarios of C_4 origin (i.e. a single gain in the ancestor of the *Bassia*/*Sedobassia*/*Camphorosma* clade with a subsequent loss in *Sedobassia* versus two independent gains in the ancestors of *Bassia* and *Camphorosma* and an independent origin of the C_3/C_4 intermediate state in *Sedobassia*) can be rejected on the basis of the phylogeny and the distribution of relevant characteristics across it. Likewise, whether there were two independent origins of a Kranz-like arrangement of chlorenchyma (in the ancestor of *Bassia* and in the ancestor of *Sedobassia*), or a single origin in the *Bassia* clade and secondary development of a continuous Kranz layer around the leaf in *Camphorosma* cannot be discerned (Fig. 3). This uncertainty can largely be blamed on the (for the purpose, unfortunately simple) shape of the phylogenetic tree. The reciprocal monophyly of three distinct C_4 and C_3/C_4 intermediate syndromes, to the exclusion of C_3 outgroups, does not allow for confident inference of the ancestral states of the clades. Our parsimony-based approach for simultaneously inferring ancestral states of both C_3/C_4 syndromes and their constituent attributes could offer a greater advantage in inferring combinations of ancestral characteristics compared with simple character optimization when used with a more tractable topology.

Irrespective of topology, the small number of character state shifts that the *Bassia* tree implies does make it unlikely that we have failed to infer further, unobserved shifts between C_3 and C_4 (i.e. homoplasy). However, it means that we also lack the statistical power necessary to support more complex likelihood models that might imply higher rates of gains or losses (Harvey and Pagel, 1991; Pirie *et al.*, 2012). Thus, the hypotheses cannot be assessed on that basis either. As the sampling of this clade is almost complete, it seems unlikely that this kind of approach will yet yield a more certain solution in this case.

Comparing the two clades that acquired the full C_4 syndrome, the genera *Bassia* and *Camphorosa*, reveals some obvious differences. The crown group age, which at the same time is the minimum age of full C_4 syndrome in these two genera, is older in *Bassia* than in *Camphorosma*, 17.1–6.4 and 10.7–3.1 million years, respectively (Fig. 2). While in *Bassia* four distinct C_4 leaf types evolved and multiple shifts between these types occur (see below; Fig. 2), species of *Camphorosma* (annuals and perennials) all show the same C_4 leaf types (Figs 1B and 2). The diversity of C_4 leaf types in *Bassia* is probably not a simple function of its greater age, because up to three different leaf types can be found even in much younger subclades (e.g. *B. scoparia* clade or *B. prostrata* clade). It seems that the ancestral leaf types in *Bassia*, which in our analysis were found to be those of *B. prostrata* and *B. muricata* (Fig. 2), allow for rapid anatomical change, while the *Camphorosma* type does not. The major difference between these types is in the arrangement of the Kranz cells, which form a continuous Kranz layer around the leaf in *Camphorosma* but are restricted to the vascular bundles in all *Bassia* leaf types (Fig. 3).

Further insight may be gained from comparative leaf developmental studies of these two genera. Similarities or differences of developmental phases of *Bassia* and *Camphorosma* leaf maturation might give further indication of common or independent ancestry of the C_4 syndrome in this lineage. The continuous arrangement of Kranz cells in mature leaves of *Camphorosma* might indicate that in this genus the Kranz cells derive from ground meristem, as in *Suaeda taxifolia* and *Suaeda eltonica* (Koteyeva *et al.*, 2011). However, the cotyledons of *Bassia hyssopifolia*, *B. prostrata*, *Bassia laniflora*, *B. scoparia*, *B. arabica*, *B. odontoptera*, *B. pilosa*, *Camphorosma songarica* and *Camphorosma lessingii* all show an atriplicoid leaf anatomy, indicating that the genetic basis for differentiation of a C_4 bundle sheath is present in both genera (G. Kadereit and H. Freitag, unpublished results). Therefore, a combined origin of the Kranz cells, partly from procambial and partly from ground tissue, as shown by Dengler *et al.* (1995) in *Atriplex*, might also be possible.

Loss of water-storage tissue in Camphorosmeae

The combination of water-storage tissue in leaves or stems and C_4 photosynthesis occurs in approximately 500 species distributed in the Asterales, Brassicales, Zygophyllales, and Caryophyllales. However, most species that combine these two traits are found within the Chenopodiaceae, in the subfamilies Suaedoideae, Salsoloideae, and Camphorosmoideae, in which succulence evolved prior to C_4. It should be emphasized that the presence of a water-storage tissue is not always obvious and might only be detected after sectioning. Several flat-leaved C_4 species might also show small amounts of tissue that could serve for water storage. There seem to be no examples of succulence having evolved within a C_4 chenopod lineage, although in some taxa succulence might have increased. This study gives the first evidence of repeated loss of water-storage tissue in an ancestrally succulent lineage after the evolution of the C_4 pathway (Fig. 3).

However, as is the case with C_3 versus C_4, the coding of presence versus absence of succulence represents a considerable simplification. Various different forms of succulence are apparent: in *Camphorosma*, the volume of the central water storage is generally comparatively small. In some populations of the perennial species, it is much reduced and is replaced by an enlarged sclerenchymatic tissue associated with the central vascular bundle, giving the leaves an almost needle-like structure. *Bassia eriantha* has lost a centrally located water-storage tissue and evolved an atriplicoid arrangement of the chlorenchyma (Fig. 2). However, in contrast to the other species with atriplicoid anatomy, *B. eriantha* shows a hypodermis consisting of cells that are greatly enlarged and obviously has taken on a water-storage function.

There are also examples of intermediate phenotypes between the *B. muricata* and *B. lasiantha* types with a rudimentary aqueous tissue as observed in *B. scoparia* (e.g. Fig. 1K) and *B. pilosa.* These intermediate phenotypes may indicate that loss of water-storage tissue happened gradually in populations growing under less severe drought regimes, although a test of whether these different stages of reduction are genetically fixed is warranted.

All species that represent independent losses of central water-storage tissue (*B. eriantha*, *B. scoparia*, *B. lasiantha*, and *B. pilosa*) are annuals with *B. eriantha*- or *B. lasiantha*-type anatomy. Irrespective of anatomical differences, this suggests that loss of succulence in these cases was associated with a shift to a drought-avoidance strategy, which is most common in arid ecosystems with strong seasonal drought (Ellenberg, 1967; Evenari, 1981, 1985).

A revised model for the evolution and homology of leaf types in Camphorosmeae

With the new insight from a more detailed and resolved phylogeny of the clade, we can somewhat qualify the previous interpretation of evolution of its leaf types (Fig. 3). The current model does not feature the unobserved, intermediate anatomical types that must have existed in ancestors of the current lineages (if we do not assume that multiple traits arose simultaneously). However, the available evidence is insufficient to identify which combinations of traits these ancestors might have had, and it is parsimonious to assume that the most recent common ancestors of the major clades exhibited combinations of characteristics also shared by extant taxa.

The presence or absence of a hypodermis, which distinguishes a number of the leaf anatomy types in Camphorosmeae, appears to be particularly evolutionarily labile. This is indicated by both the relatively high rate of shifts in this character and the observation of intermediate phenotypes in both *B. prostrata*/*B. muricata* and *B. muricata*/*B. lasiantha* types (Fig. 1G, H, J; Freitag and Kadereit, 2014). Variability in the presence/absence of hypodermis is also apparent in other Chenopodiaceae lineages, including *Atriplex*, Salsoleae s.s., Caroxyloneae, and *Suaeda* (Kadereit *et al.*, 2003). The *B. eriantha* type with its water-storing hypodermis is, for example, similar to the *Schoberia* type described from genus *Suaeda* (Schütze *et al.* 2003). Given the high rate of shifts in this

character, it is not possible to discern between *B. muricata* and *B. prostrata* types as the progenitors of *B. eriantha* or *B. lasiantha* types. However, it is notable that the perennial, woody species all exhibit a hypodermis, while in most annual species it is lacking. If the possession of a hypodermis, which is present in all perennial C_4 species of Camphorosmeae, is the ancestral condition, as would be implied by homology with the outer chlorenchyma layer of C_3 species, then its multiple loss might be associated with the shift to annual life form. However, from these analyses it is still unclear whether or not the hypodermis in C_4 species should be considered homologous to the outer chlorenchyma layer of C_3 species or not. The only C_3/C_4 intermediate species in Camphorosmeae, *Sedobassia sedoides*, is uninformative in this regard because it shows a C_3-like multilayered chlorenchyma. In future work, the homology and hence evolutionary significance of the hypodermis may be analysed more effectively in a broader phylogenetic context (e.g. Chenopodiaceae as a whole) that represents a larger number of apparent gains and/or losses and perhaps a clearer indication of the ancestral condition in each case.

Conclusions and future research

This work shows that a deep study including a fully sampled and resolved phylogenetic tree of the study group as well as detailed and complete assessment of anatomical traits reveals a somewhat more complex picture of C_4 leaf-type evolution as compared with our previous work. In the case of *Bassia*, we confirmed multiple parallel shifts between C_4 leaf types due to losses of water-storage tissue and losses (and/or gains) of the hypodermis. In this genus, it is clear that different C_4 leaf types are not necessarily indicative of independent C_4 origins. They instead point to a rapid change of leaf anatomy in adaptation to different survival strategies in steppic or semi-desert habitats. *Camphorosma* differs from *Bassia* in showing a fixed C_4 anatomy differing from all *Bassia* types in having a continuous Kranz layer. In contrast to anatomical differences defined by aqueous tissue and the hypodermis, this distinct structural difference might indeed point to an independent origin of the full C_4 syndrome in *Camphorosma*, either from an independent C_3 or from a common C_3/C_4 intermediate ancestor.

On the basis of the phylogeny and character distribution, we cannot exclude a single gain of C_4 in the ancestor of the *Bassia*/*Sedobassia*/*Camphorosma* clade and a subsequent loss in *Sedobassia*. However, given the anatomical differentiation and the distribution of *Sedobassia* in similar habitats as *Bassia* and *Camphorosma*, the scenario avoiding loss of C_4-like structures as suggested by Freitag and Kadereit (2014) seems more likely. Such a scenario could either involve two independent gains of C_4 in the ancestors of *Bassia* and *Camphoroma* and an independent origin of the C_3/C_4 intermediate state in *Sedobassia* or a common C_3/C_4 intermediate ancestor for *Bassia*/*Sedobassia*/*Camphorosma* clade and subsequent independent further acquisition of a different full C_4 syndrome in *Bassia* and *Camphorosma*. In the former case, *Sedobassia* would represent the ancestral state of an ancient C_3/C_4 intermediate, while in the latter it would represent a derived, more recent syndrome. In both cases, the C_3/C_4 intermediate anatomy in *Sedobassia* with enlarged bundle sheath cells shows that, in ancestrally succulent lineages, bundle-sheath enlargement might also be an important step on the path towards C_4 evolution.

In future research, the analytical approaches used here—phylogenetic inference and model testing—are likely to be more powerful when applied to a wider phylogeny, including more examples of particular state shifts, and across multiple relevant plant groups. However, broad-scale inference approaches should be complemented by both detailed studies of individual clades and by experimental testing of hypotheses. Camphorosmeae represent a promising system with which to investigate parallel evolution of anatomical traits at the ultrastructural level and in terms of gene expression. To go beyond observation and inference and directly test the selective advantage of traits, it would be useful to compare the ecophysiological performance of sister species with different leaf anatomies under particular ecological conditions (such as degrees of drought, salinity, and atmospheric CO_2 concentration). In this context, it would also be interesting to quantify the amount of aqueous tissue and relate it to the ecophysiological performance of the species.

Supplementary data

Supplementary data are available at *JXB* online.

Supplementary Table S1. Accessions included in the molecular and anatomical analyses with lab code, voucher information, Genbank accession numbers and leaf anatomical types.

Supplementary Table S2. PCR conditions and primer sequences for the four markers sequenced in this study.

Supplementary Table 3. Character coding for 79 accessions of Camphorosmeae and *Salsola genistoides* (outgroup from Salsoleae s.s).

Supplementary Fig. S1. Molecular phylogeny of Camphorosmeae based on sequences of the internal transcribed spacer (ITS) analysed with a maximum-likelihood approach using RaxML on Cipres (Stamatakis, 2006; Stamatakis *et al.*, 2008).

Supplementary Fig. S2. Molecular phylogeny of Camphorosmeae based on sequences of three non-coding cp markers (atpB-rbcL spacer, rpl16 intron, and ndhF-rpl32 spacer) analysed with a maximum-likelihood approach using RaxML on Cipres (Stamatakis, 2006; Stamatakis *et al.*, 2008).

Supplementary Fig. S3. Molecular phylogeny of Camphorosmeae based on sequences of the internal transcribed spacer (ITS) and three non-coding cp markers (atpB-rbcL spacer, rpl16 intron, and ndhF-rpl32 spacer) analysed with a maximum-likelihood approach using RaxML on Cipres (Stamatakis, 2006; Stamatakis *et al.*, 2008).

Supplementary Fig. S4. Step matrices representing the number of character state changes implied by shifts between each pair of states (including those not observed in extant taxa).

Acknowledgements

We are grateful to all colleagues who contributed material to this study. We thank Zaid Altarada (Hebron) and Silvia Wienken (Mainz) for their help in the laboratory, and Lisa Wernet (Mainz) for her assistance with the leaf sectioning. We thank Doris Franke (Mainz) for her help with the figures. We gratefully acknowledge the comments of Elena Voznesenskaya (St Petersburg) and one anonymous reviewer. We thank the German Science foundation (DFG; grant to GK) and the Johannes Gutenberg-Universität Mainz for financial support.

References

Akhani H, Khoshravesh R. 2013. The relationship and different C_4 Kranz anatomy of *Bassia eriantha* and *Bassia eriophora*, two often confused Irano-Turanian and Saharo-Sindian species. *Phytotaxa* **93,** 1–24.

Bellstedt DU, Galley C, Pirie MD, Linder HP. 2012. Migration of the palaeotropical arid flora: Zygophylloideae as an example. *Systematic Botany* **37,** 951–959.

Blattner FR. 1999. Direct amplification of the entire ITS region from poorly preserved plant material using recombinant PCR. *BioTechniques* **27,** 1180–1186.

Cabrera J, Jacobs SWL, Kadereit G. 2011. Biogeography of Camphorosmeae (Chenopodiaceae): tracking the Tertiary history of Australian aridification. *Telopea* **13,** 313–326.

Christin PA, Besnard G, Samartitani E, Duvall MR, Hodkinson TR, Savolainen V, Salamin N. 2008. Oligocene CO_2 decline promoted C_4 photosynthesis in grasses. *Current Biology* **18,** 37–43.

Christin PA, Freckleton RP, Osborne CP. 2010. Can phylogenetics identify C_4 origins and reversals? *Trends in Ecology and Evolution* **25,** 403–409.

Christin PA, Osborne CP. 2013. The recurrent assembly of C_4 photosynthesis, an evolutionary tale. *Photosynthesis Research* **117,** 163–175.

Christin PA, Osborne CP, Chatelet DS, Columbus IT, Besnard G, Hodkinson T, Garrison LM, Vorontsova, MS, Edwards EJ. 2013. Anatomical enablers and the evolution of C_4 photosynthesis in grasses. *Proceedings National Academy of Sciences USA* **110,** 1381–1386.

Dengler NG, Dengler RE, Donnelly PM, Filosa M. 1995. Expression of the C_4 pattern of photosynthetic enzyme accumulation during leaf development in *Atriplex rosea* (Chenopodiaceae). *American Journal of Botany* **82,** 318–327.

Drummond AJ, Rambaut A. 2007. BEAST: Bayesian evolutionary analysis by sampling trees. *BMC Evolutionary Biology* **7,** 214.

Edwards EJ, Smith SA. 2010. Phylogenetic analyses reveal the shady history of C_4 grasses. *Proceedings National Academy of Sciences USA* **107,** 2532–2537.

Edwards GE, Voznesenskaya EV. 2011. C_4 photosynthesis: Kranz forms and single-cell C_4 in terrestrial plants. In: Raghavendra AS, Sage RS, eds. C_4 photosynthesis and related CO_2 concentrating mechanisms. Dordrecht, The Netherlands: Springer Science+Business Media B.V., 29–61.

Ellenberg H. 1967. A key to Raunkiaer plant life forms with revised subdivisions. *Bulletin of the Geobotanical Institute ETH* **37,** 56–73.

Evenari M. 1981. Synthesis. In: Goodall DW, Perry RA, Howes KMW, eds. *Arid-land ecosystems: structure, functioning and management*. Cambridge, UK: Cambridge University Press, 555–591.

Evenari M. 1985. Adaptations of plants and animals to the desert environment. In: Evenari M, Noy-Meir I, Goodall DW, eds. *Hot deserts and arid shrublands. Ecosystems of the World 12A*. Amsterdam, The Netherlands: Elsevier, 79–92.

Freitag H, Kadereit G. 2014. C_3 and C_4 leaf anatomy types in Camphorosmeae (Camphorosmoideae, Chenopodiaceae). *Plant Systematics and Evolution*. **300,** 665–687.

Griffiths H, Weller G, Toy LFM, Dennis RJ. 2013. You're so vein: bundle sheath physiology, phylogeny and evolution in C_3 and C_4 plants. *Plant, Cell & Environment* **36,** 249–261.

Harvey PH, Pagel M. 1991. *The comparative method in evolutionary biology*. Oxford, UK: Oxford University Press.

Jürgens N. 1997. Floristic biodiversity and history of African arid regions. *Biodiversity and Conservation* **6,** 495–514.

Kadereit G, Borsch T, Weising K, Freitag H. 2003. Phylogeny of Amaranthaceae and Chenopodiaceae and the evolution of C_4 photosynthesis. *International Journal of Plant Science* **164,** 959–986.

Kadereit G, Freitag H. 2011. Molecular phylogeny of Camphorosmeae (Camphorosmoideae, Chenopodiaceae): implications for biogeography, evolution of C_4 photosynthesis and taxonomy. *Taxon* **60,** 51–78.

Kadereit G, Ackerly D, Pirie MD. 2012. A broader model for C_4 evolution in plants inferred from the goosefoot family (Chenopodiaceae s.s.). *Proceedings of the Royal Society of London B: Biological Sciences* **279,** 3304–3311.

Kapralov MV, Akhani H, Voznesenskaya EV, Edwards G, Franceschi V, Roalson EH. 2006. Phylogenetic relationships in the Salicornioideae/Suaedoideae/Salsoloideae s.l. (Chenopodiaceae) clade and a clarification of the phylogenetic position of *Bienertia* and *Alexandra* using multiple DNA sequence datasets. *Systematic Botany* **31,** 571–585.

Koteyeva NK, Voznesenskaya EV, Berry JO, Chuong SDX, Franceschi VR, Edwards GE. 2011. Development of structural and biochemical characteristics of C_4 photosynthesis in two types of Kranz anatomy in genus *Suaeda* (family Chenopodiaceae). *Journal of Experimental Botany* **62,** 3197–3212.

Marazzi B, Ané C, Simon MF, Delgado-Salinas A, Luckow M, Sanderson MJ. 2012. Locating evolutionary precursors on a phylogenetic tree. *Evolution* **66,** 3918–3930.

McKown AD, Dengler NG. 2007. Key innovations in the evolution of Kranz anatomy and C_4 vein pattern in *Flaveria* (Asteraceae). *American Journal of Botany* **94,** 382–399.

Müller K. 2005. The efficiency of different search strategies in estimating parsimony jackknife, bootstrap, and Bremer support. *BMC Evolutionary Biology* **5,** 58.

Osborne CP, Beerling DJ. 2006. Nature's green revolution: the remarkable evolutionary rise of C_4 plants. *Philosophical Transactions of the Royal Society Series B* **361,** 173–194.

Osborne CP, Freckleton RP. 2009. Ecological selection pressures for C_4 photosynthesis in the grasses. *Proceedings of the Royal Society of London B: Biological Sciences* **276,** 1753–1760.

Pirie MD, Humphreys AM, Antonelli A, Galley C, Linder HP. 2012. Model uncertainty in ancestral area reconstruction: a parsimonious solution? *Taxon* **61,** 652–664.

Rambaut A, Drummond AJ. 2003. Tracer v. 1.5. (1.3 edn). Available at: http://beast.bio.ed.ac.uk/Tracer.

Sage RF. 2001. Environmental and evolutionary preconditions for the origin and diversification of the C_4 photosynthetic syndrome. *Plant Biology* **3,** 202–213.

Sage RF, Christin PA, Edwards EJ. 2011. The C_4 plant lineages of planet Earth. *Journal of Experimental Botany* **62,** 3155–3169.

Sage RF, Sage TL, Kocacinar F. 2012. Photorespiration and the evolution of C_4 photosynthesis. *Annual Review of Plant Biology* **63,** 19–47.

Sage RF, Khoshravesh R, Sage TL. 2014. From proto-Kranz to C4 Kranz: building the bridge to C4 photosynthesis. *Journal of Experimental Botany* **65,** 000–000.

Schütze P, Freitag H, Weising K. 2003. An integrated molecular and morphological study on Suaedoideae Ulbr. (Chenopodiaceae). *Plant Systematics and Evolution* **239,** 257–286.

Snijman DA, Manning JC. 2013. *Chenolea convallis*, a new species from Western Cape Province, South Africa. *Bothalia* **43,** 80–84.

Stamatakis A. 2006. RAxML-VI-HPC: Maximum likelohood-based phylogenetic analyses with thousands of taxa and mixed models. *Bioinformatics* **22,** 2688–2690.

Stamatakis A, Hoover P, Rougemont J. 2008. A fast bootstrapping algorithm for the RAxML web-servers. *Systematic Biology* **57,** 758–771.

Swofford DL. 2003. PAUP*: phylogenetic analysis using parsimony (*and other methods), version 4. Sinauer Associates, Sunderland, Massachusetts.

Tamura K, Peterson D, Peterson N, Stecher G, Nei M, Kumar S. 2011. MEGA5: molecular evolutionary genetics analysis using maximum likelihood, evolutionary distance, and maximum parsimony methods. *Molecular Biology and Evolution* **28,** 2731–2739.

Verdcourt B. 1969. The arid corridor between the north-east and south-west areas of Africa. In: van Zinderen-Bakker EM, ed. *Paleoecology of Africa*. Cape Town, South Africa: Balkema, 140–144.

Voznesenskaya EV, Koteyeva NK, Akhani H, Roalson EH, Edwards GE. 2013. Structural and physiological analyses in Salsoleae (Chenopodiaceae) indicate multiple transitions among C_3, intermediate, and C_4 photosynthesis. *Journal of Experimental Botany* **64,** 3583–3604.

White TJ, Bruns T, Lee S, Taylor JW. 1990. Amplification and direct sequencing of fungal ribosomal RNA genes for phylogenetics. In: Innis MA, Gelfand DH, Sninsky JJ, White TJ, eds. *PCR protocols: a guide to methods and applications*. NewYork: Academic Press, 315–322.

Wilgenbusch JC, Warren DL, Swofford DL. 2004. AWTY: a system for graphical exploration of MCMC convergence in Bayesian phylogenetic inference. Available at: http://king2.scs.fsu.edu/CEBProjects/awty/awty_start.php.